

# Sub-Picosecond Singlet Exciton Fission in Cyano-Substituted Diaryltetracenes\*\*

Eric A. Margulies, Yi-Lin Wu, Przemyslaw Gawel, Stephen A. Miller, Leah E. Shoer, Richard D. Schaller, François Diederich,\* and Michael R. Wasielewski\*

**Abstract:** Thin films of 5,11-dicyano-6,12-diphenyltetracene (TcCN) have been studied for their ability to undergo singlet exciton fission (SF). Functionalization of tetracene with cyano substituents yields a more stable chromophore with favorable energetics for exoergic SF ( $2E(T_1) - E(S_1) = -0.17$  eV), where  $S_1$  and  $T_1$  are singlet and triplet excitons, respectively. As a result of tuning the triplet-state energy, SF is faster in TcCN relative to the corresponding endoergic process in tetracene. SF proceeds with two time constants in the film samples ( $\tau = 0.8 \pm 0.2$  ps and  $\tau = 23 \pm 3$  ps), which is attributed to structural disorder within the film giving rise to one population with a favorable interchromophore geometry, which undergoes rapid SF, and a second population in which the initially formed singlet exciton must diffuse to a site at which this favorable geometry exists. A triplet yield analysis using transient absorption spectra indicates the formation of  $1.6 \pm 0.3$  triplets per initial excited state.

The possibility of increasing the quantum yield of charge-carrier generation through singlet exciton fission (SF), whereby one singlet exciton ( $S_1$ ) is energetically downcon-

verted to two long-lived triplet excitons, has attracted much attention recently, especially in the field of organic photovoltaics (OPVs).<sup>[1]</sup> Systems displaying quantitative SF have been shown theoretically to increase the thermodynamic limit of single junction photovoltaics to 45 %, far above the 32 % Shockley–Queisser limit.<sup>[2]</sup> Recent efforts to harvest the resultant triplets from SF in nanocrystalline inorganic semiconductors<sup>[3]</sup> and in OPV devices<sup>[4]</sup> have demonstrated that collection can be rapid and highly efficient.

The SF process can be rapid (sub-picosecond) as the formation of two triplet excitons proceeds through a spin-allowed, correlated triplet pair, denoted  $^1(TT)$ . The actual SF rate depends heavily on two factors: energetics and intermolecular electronic coupling. Exoergic SF, where twice the triplet exciton energy is less than the lowest singlet exciton energy ( $E(S_1) \geq 2E(T_1)$ ), favors high-yielding, rapid SF.<sup>[5]</sup> Michl and Nakano and co-workers have suggested that this somewhat uncommon energetic scenario is facilitated by structures that have some degree of biradical character in their lowest singlet state.<sup>[1,6]</sup> Additionally, theory predicts that a slip-stacked motif provides better electronic coupling than perfectly face-to-face  $\pi$ -stacked chromophores.<sup>[1]</sup>

Tetracene and its derivatives have been the focus of many experimental and theoretical studies<sup>[7]</sup> as the parent chromophore undergoes SF with a high triplet quantum yield (up to 200 %); however, poor solubility and photoinstability have hindered practical applications. Arylation of tetracene improves its solubility and modulates crystal packing, but does little to improve its stability towards oxygen.<sup>[8]</sup> On the other hand, substitution with cyano groups has been found to greatly improve its stability.<sup>[9]</sup> This results in a chromophore that is both soluble and stable in chloroform solution over months, whereas phenyl-substituted derivatives, such as rubrene, decompose after a few days in solution.

Recently, a method has been developed for preparing a series of cyano-substituted diaryltetracenes through a cascade reaction comprising [2+2] cycloaddition, retroelectrocyclization, and electrocyclization of tetraaryl [3]cumulene with tetracyanoethene (TCNE), followed by formal elimination of cyanogen.<sup>[10]</sup> The resultant 5,11-dicyano-6,12-diphenyltetracene (TcCN) displays high stability in solution and in the solid state. The molecule crystallizes in the  $P\bar{1}$  space group with one half molecule per asymmetric unit, forming infinite  $\pi$  stacks that are slip-stacked along both the long and short axes (Figure 1). DFT calculations (B3LYP/6-31G(d)) suggest that this chromophore exceeds the energetic requirements for SF by a wide margin. This is in contrast to tetracene ( $2E(T_1) - E(S_1) = 0.18$  eV)<sup>[7]</sup> and its arylated deriv-

[\*] E. A. Margulies, Dr. Y.-L. Wu, Dr. S. A. Miller, Dr. L. E. Shoer, Prof. Dr. M. R. Wasielewski  
Department of Chemistry and Argonne-Northwestern Solar Energy Research (ANSER) Center, Northwestern University  
2145 Sheridan Road, Evanston, IL 60208 (USA)  
E-mail: m-wasielewski@northwestern.edu

Prof. Dr. R. D. Schaller  
Department of Chemistry  
Northwestern University and Center for Nanoscale Materials  
Argonne National Laboratory, Argonne, IL 60439 (USA)

P. Gawel, Prof. Dr. F. Diederich  
Laboratorium für Organische Chemie, ETH Zürich  
Vladimir-Prelog-Weg 3, HCI, 8093 Zürich (Switzerland)  
E-mail: diederich@org.chem.ethz.ch

[\*\*] This work was supported by the Chemical Sciences, Geosciences, and Biosciences Division, Office of Basic Energy Sciences, U.S. Department of Energy (DOE), under Grant No. DE-FG02-99ER14999 (M.R.W.), the Swiss National Science Foundation, and the ERC Advanced Grant No. 246637 ("OPTELOMAC"). This work was performed, in part, at the Center for Nanoscale Materials, a U.S. Department of Energy, Office of Science, Office of Basic Energy Sciences User Facility under Contract No. DE-AC02-06CH11357. This work made use of the J. B. Cohen X-ray Diffraction Facility at the Materials Research Center of Northwestern University supported by the National Science Foundation MRSEC program (DMR-1121262). We thank Dr. Matthew Krzyaniak and Dr. Samuel Eaton for help with data analysis, acquiring time-resolved fluorescence data, and helpful discussions.

Supporting information for this article is available on the WWW under <http://dx.doi.org/10.1002/anie.201501355>.

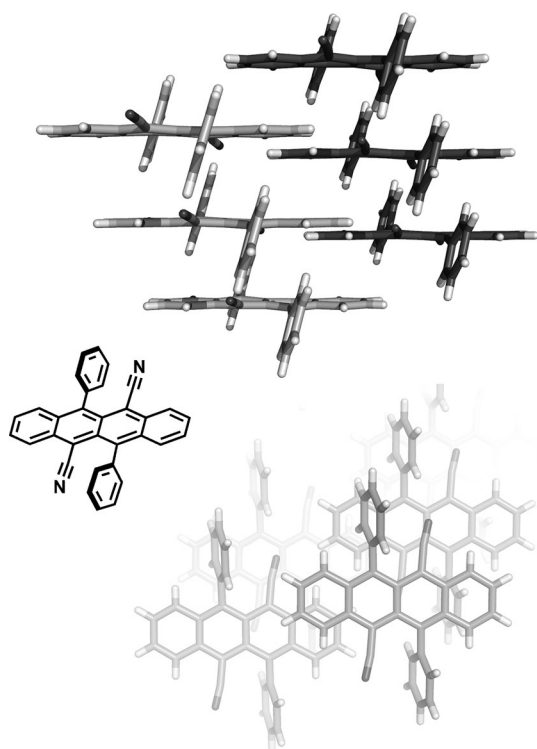


**Figure 1.** Chemical structure of **TcCN** (left) and two views of the packing of **TcCN** within its crystal structure (top and bottom).<sup>[10]</sup>

atives (for example, 0.07 eV for rubrene),<sup>[11]</sup> where SF is thermally activated or requires an entropic contribution.<sup>[12]</sup>

The favorable characteristics of **TcCN** motivated us to examine its potential as a candidate for SF. Using femto-second transient absorption spectroscopy (fsTA), we compare the photophysics of **TcCN** measured in solution to those measured in thin-film samples (see the Supporting Information). Photoexcitation of the solution samples at  $\lambda = 500$  nm yields a transient absorption signal consistent with excited-state absorption. Most notably, an  $S_n \leftarrow S_1$  excited-state absorption (ESA) is detected with a band at  $\lambda = 489$  nm, in addition to a ground state bleach (GSB) feature at 545 nm and a stimulated emission (SE) feature at 600 nm. An additional ESA feature detected in the near-infrared (NIR) region, centered at  $\lambda = 1280$  nm, is far removed from the GSB.

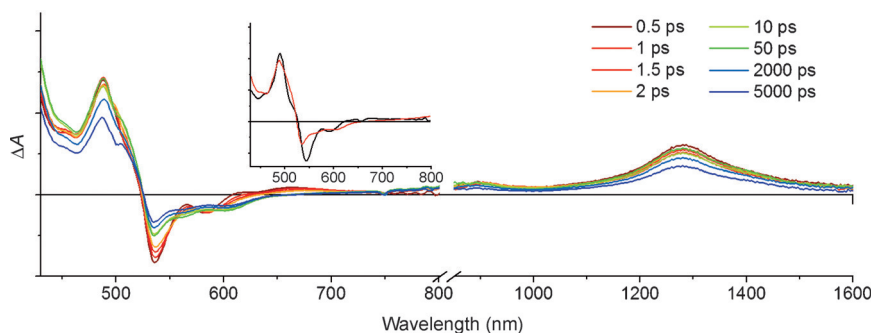


**Figure 2.** Visible and NIR fsTA spectra of **TcCN** in  $\text{CH}_2\text{Cl}_2$  solution. Inset: Species-associated spectra of the initial singlet excited state (black) and the structurally-relaxed singlet excited state (red).

The kinetics of this ESA band are biexponential ( $\tau_1 = 2.4 \pm 0.1$  ps and  $\tau_2 = 11.5 \pm 0.1$  ns) at all wavelengths in the visible region of the spectrum. Species-associated spectra (Figure 2, inset) obtained by singular value decomposition (SVD) and global target analysis of the three-dimensional absorption change ( $\Delta A$ ) versus time and wavelength data set show that the spectral differences between the initial species (black line) and the longer-lived species (red line) result from both a blue-shift of the ESA (which is strongly overlapped with the GSB around  $\lambda = 540$  nm) and a red-shift of the SE (around 600 nm). The faster process corresponds to structural relaxation of the excited state, in agreement with the relatively large Stokes shift measured in solution.<sup>[10]</sup> Furthermore, a sample of **TcCN** in a rigid polystyrene matrix exhibited a decreased rate of structural relaxation (see the Supporting Information and Figures S2 and S3 for further analysis of the structural relaxation).

These solution data reveal a long-lived singlet excited state, which implies that any inherent triplet formation by intersystem crossing (ISC) is quite slow. Based on the quantum yield of fluorescence ( $\phi_f$ ) and the excited state lifetime ( $\tau_{\text{NR}}$ , where NR = nonradiative), a lower limit to the ISC time constant ( $\tau_{\text{ISC}} = \tau_{\text{NR}}$ ) is found by Equation (1) to be 19 ns. Based on the near absence of any long-lived species in the solution transient absorption spectrum, it is likely that this lifetime is even longer. Additionally, this long-lived excited singlet state suggests that any rapid photophysical process, such as SF, will not be in kinetic competition with other singlet quenching pathways available to the molecule.

$$\tau_{\text{NR}} = \frac{\tau_s}{1 - \phi_f} \quad (1)$$

To study SF in the solid state, **TcCN** was vapor deposited onto heated (363 K, HT) and room temperature (295 K, RT) glass substrates to yield 140 and 116 nm thick films, respectively. Rapid deposition onto RT substrates results in a lower degree of crystallinity, as evidenced by a broad amorphous scattering peak in the grazing incidence X-ray diffraction data (see Figure S1 in the Supporting Information). This film also exhibits significantly lower Rayleigh scattering, as detected in the transmission-only absorption spectrum, which is consistent with the presence of smaller crystallites in the RT film.

The scatter-corrected absorption spectrum of the RT film is very similar to the solution spectrum except for an 11 nm red-shift of the vibronic bands in the solid, and a small enhancement of the 0–1 and 0–2 vibronic band intensities relative to the 0–0 vibronic band (Figure 3). The red-shift of the 0–0 band indicates that the  $S_1$  state is slightly more stable in the solid (2.25 eV) relative to solution (2.28 eV). These changes are consistent with a mixed population of molecules having relatively weak interchromophore H- and J-type transition dipole couplings as predicted by exciton theory.<sup>[13]</sup> In the HT film, the 0–1 and 0–2 vibronic band intensities are

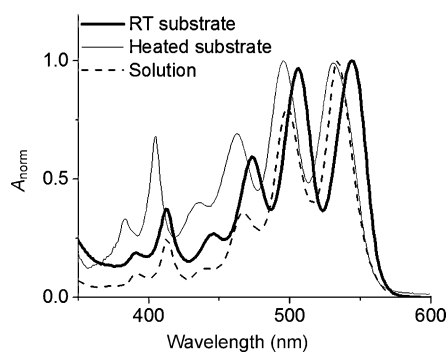


**Figure 3.** Normalized absorption spectrum of **TcCN** in  $\text{CH}_2\text{Cl}_2$  solution (dashed) and normalized scatter-corrected absorption spectra of thin-film samples evaporated on heated (HT; thin solid line) and room temperature (RT; thick solid line) substrates.

enhanced somewhat more relative to the 0–0 vibronic band and are blue-shifted, which is indicative of a higher population of chromophores having H-type transition dipole coupling. Again, these effects are consistent with relatively modest interchromophore coupling.

Phosphorescence measurements on the RT film (Figure S4) revealed a triplet emission band centered at  $\lambda = 1190$  nm (1.04 eV). This result is in agreement with our calculations and confirms that SF is exoergic in **TcCN** ( $2E(\text{T}_1) - E(\text{S}_1) = 2 \times 1.04 \text{ eV} - 2.25 \text{ eV} = -0.17 \text{ eV}$ ) as a result of a significant lowering of the triplet excited-state energy compared to tetracene. This lowering of the  $\text{T}_1$  energy is likely related to the stabilization of the open-shell electronic configuration by the cyano functional group, as supported by the  $\text{T}_1$  state spin-density distribution (Table S1).

The fsTA spectra of the RT film following excitation at  $\lambda = 500$  nm are shown in Figure 4a. The film demonstrates rapid decay of an initial singlet excited state with an ESA band around 580 nm and an SE band centered around 605 nm. These bands decay completely within 50 ps concomitant with the appearance of transient signals strongly resembling those of the tetracene triplet excited state with an absorption band centered around  $\lambda = 560$  nm.<sup>[7d,h]</sup> The assignment of this new feature to the triplet state is further supported by triplet sensitization experiments using palladium octabutoxyphthalocyanine as a dopant in the film (Figure S6). Additionally, the dynamics remain entirely unchanged over a wide range of excitation densities (between approximately  $10^{17}$ – $10^{19}$  excitons  $\text{cm}^{-3}$ ), suggesting this triplet formation process outcompetes singlet–singlet annihilation, even at higher pump fluences. Nanosecond transient absorption measurements on the RT film show that the triplet state decays

with multiexponential kinetics (Figure S5), with  $\tau_1 = 60 \pm 1$  ns (77 %),  $\tau_2 = 740 \pm 10$  ns (19 %), and  $\tau_3 = \text{infinite}$  (4 %).

In the visible fsTA data, biexponential dynamics are detected at early delay times ( $\tau_1 = 0.8 \pm 0.2$  ps,  $\tau_2 = 23 \pm 3$  ps) followed by the long-lived spectral feature attributed to  $\text{T}_\text{N} \leftarrow \text{T}_1$  absorption. Fluorescence upconversion measurements (Figure S8) on the same film yield a biexponential fluorescence decay (Figure S8;  $\tau_1 = 1.5 \pm 0.5$  (72 %) and  $\tau_2 = 13 \pm 5$  ps (28 %)). The error bars on the fit to the fluorescence decay data are wide because the signal-to-noise ratio is low as a result of the very weak fluorescence from the film. Nevertheless, these fluorescence decay lifetimes approximately match the measured decay kinetics of the  $\text{S}_1$  ESA signals as well as the growth of the  $\text{T}_1$  ESA signal in the fsTA data (Figure 4).

These two singlet-state lifetimes and the corresponding decay-associated spectra obtained by SVD and global analysis (Figure S7) suggest that the two short lifetimes result from two different SF rates. The decay-associated spectra of these two processes are strikingly similar with a negative band centered at  $\lambda = 560$  nm, corresponding to the growth of a positive  $\text{T}_\text{N} \leftarrow \text{T}_1$  absorption, and a negative band around 605 nm, corresponding to the simultaneous decay of stimulated emission as the  $\text{S}_1$  state is depopulated. Furthermore, as the  $\text{S}_1$  state is depopulated, the ESA in the NIR spectral region decays with the same rapid biexponential time constants as measured in the red spectral region within experimental error ( $\tau_1 = 0.7 \pm 0.2$  ps,  $\tau_2 = 33 \pm 7$  ps).

This biexponential depopulation of the singlet state in conjunction with a growth of the triplet-state absorption indicates that triplet-state formation by SF proceeds through

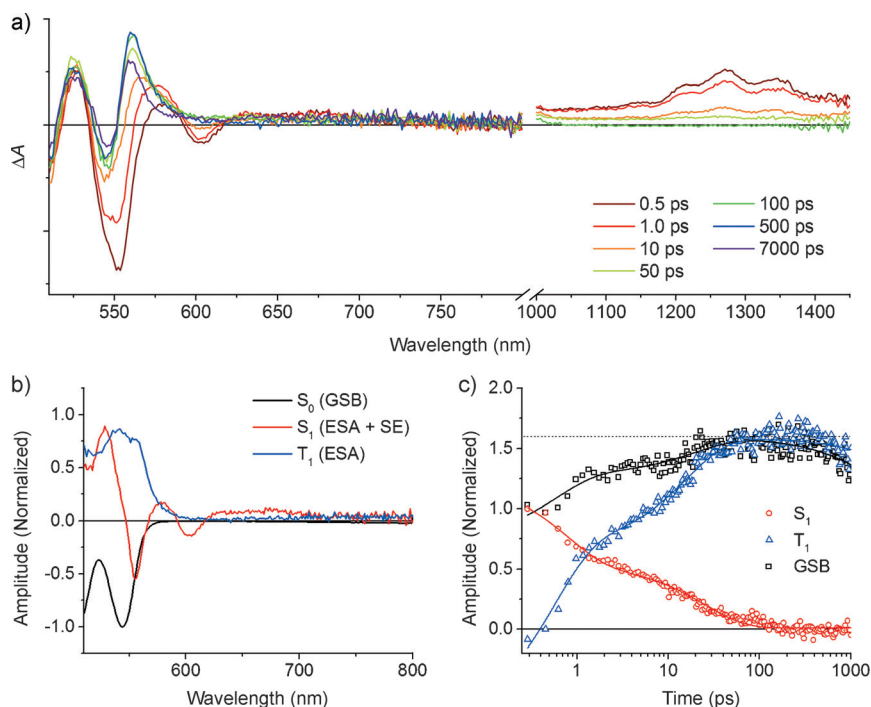


**Figure 4.** a) Visible and NIR fsTA spectra of a **TcCN** thin film deposited on a RT substrate excited at  $\lambda = 500$  nm. For clarity, NIR bands after 100 ps are not shown. b) Basis spectra used to reconstruct the transient absorption data set. c) Time-correlated amplitudes from deconvolution of the transient absorption data.



two distinct pathways. As the SF process in this chromophore is exoergic by approximately 0.2 eV, it is unlikely that rapid SF occurs from a hot vibrational state in competition with slower vibrational cooling, which subsequently yields slower SF, as has been previously found in rubrene single crystals and 1,3-diphenyl-isobenzofuran thin films.<sup>[14]</sup> Instead, we attribute the two SF time constants to structural disorder within the RT film giving rise to one population with a favorable interchromophore geometry, which undergoes rapid SF, and a second population in which the initially formed singlet exciton must diffuse to a site at which this favorable geometry exists, as has been suggested previously.<sup>[7b]</sup> In this situation, it is assumed that a wide range of interchromophore geometries and thus, intermolecular couplings, exist in the film.

To further corroborate these findings and to determine the SF efficiency, a triplet yield analysis was performed by modeling the full TA data set using a linear combination of basis spectra (Figure 4b) obtained by reconstruction of the species absorbance spectra<sup>[15]</sup> from the transient absorption data (see the Supporting Information, Figure S10). This analysis shows the formation of  $1.6 \pm 0.3$  triplets per singlet excited state, indicating triplet formation results from SF, the only process by which one singlet exciton can produce more than one triplet.

The complex nature of the SF dynamics and the lower signal-to-noise ratio of the more scattering HT film preclude accurate global analysis; however, analysis by single-wavelength kinetic fitting is sufficiently revealing. In particular, the kinetics of the GSB at  $\lambda = 555$  nm, the  $T_N \leftarrow T_1$  absorption at 570 nm, and the singlet ESA in the NIR region at 1260 nm are useful for fitting the SF dynamics. In the visible fsTA spectrum, there is a biexponential growth of the GSB ( $\tau_1 = 0.7 \pm 0.3$  ps,  $\tau_2 = 13 \pm 4$  ps) which mirrors a similar growth of the triplet ESA. This biexponential process is, once again, corroborated by the decay ( $\tau_1 = 0.8 \pm 0.3$  ps,  $\tau_2 = 16 \pm 5$  ps) of the ESA in the NIR region. In comparing the biexponential nature of the RT and HT thin films, the initial SF time constant of approximately 800 fs is unchanged; however, the longer time constant is halved in the HT film. However, the relative amplitudes of the fast and slow SF processes are consistent between films. These results suggest that the density of active sites that undergo rapid SF in the HT film does not increase, but rather, the diffusion-limited SF process is facilitated by increased crystallinity. This increase could be the result of an increased effective diffusion rate because of increased long-range order in the more crystalline sample.

In conclusion, the addition of cyano substituents is found to lower the triplet energy of tetracene, while maintaining its lowest excited singlet energy. This stabilization of the triplet state results in a triplet energy of 1.04 eV, which is close to the optimal triplet energy for SF device efficiency and in a useful range for charge injection into organic semiconductors.<sup>[3]</sup> In addition to the stabilization of the triplet state by synthetic modification, the steric bulk of the chromophore affords a packing motif that sufficiently separates molecules to prevent dramatic stabilization or Davydov splitting of the singlet in the solid state. As a result of these effects, SF is exoergic by 0.17 eV in TcCN films. This results in sub-picosecond SF, which is much more rapid than in unsubsti-

tuted tetracene. It is also found that the distribution of intermolecular geometries within the evaporated thin films gives rise to a secondary, exciton-diffusion-limited SF rate. Even so, this secondary 15–30 ps SF process also proceeds more rapidly than SF in tetracene (80 ps). In further pursuing these stable and exoergic SF chromophores, we plan to determine how functionalization of the parent compound affects the SF process as a result of steric and electronic changes. Additionally, the cyano functional group may offer a spectral probe with which to examine the SF process by time-resolved vibrational spectroscopy.

**Keywords:** chromophores · photophysics · singlet fission · tetracene derivatives · time-resolved spectroscopy

**How to cite:** *Angew. Chem. Int. Ed.* **2015**, *54*, 8679–8683  
*Angew. Chem.* **2015**, *127*, 8803–8807

- [1] M. B. Smith, J. Michl, *Chem. Rev.* **2010**, *110*, 6891–6936.
- [2] M. C. Hanna, A. J. Nozik, *J. Appl. Phys.* **2006**, *100*, 074510.
- [3] a) M. Tabachnyk, B. Ehrler, S. Gélinas, M. L. Böhm, B. J. Walker, K. P. Musselman, N. C. Greenham, R. H. Friend, A. Rao, *Nat. Mater.* **2014**, *13*, 1033–1038; b) N. J. Thompson, M. W. B. Wilson, D. N. Congreve, P. R. Brown, J. M. Scherer, T. S. Bischof, M. Wu, N. Geva, M. Welborn, T. V. Voorhis, V. Bulović, M. G. Bawendi, M. A. Baldo, *Nat. Mater.* **2014**, *13*, 1039–1043.
- [4] D. N. Congreve, J. Lee, N. J. Thompson, E. Hontz, S. R. Yost, P. D. Reusswig, M. E. Bahlke, S. Reineke, T. Van Voorhis, M. A. Baldo, *Science* **2013**, *340*, 334–337.
- [5] S. R. Yost, J. Lee, M. W. B. Wilson, T. Wu, D. P. McMahon, R. R. Parkhurst, N. J. Thompson, D. N. Congreve, A. Rao, K. Johnson, M. Y. Sfeir, M. G. Bawendi, T. M. Swager, R. H. Friend, M. A. Baldo, T. Van Voorhis, *Nat. Chem.* **2014**, *6*, 492–497.
- [6] T. Minami, M. Nakano, *J. Phys. Chem. Lett.* **2011**, *3*, 145–150.
- [7] a) R. E. Merrifield, P. Avakian, R. P. Groff, *Chem. Phys. Lett.* **1969**, *3*, 155–157; b) Y. Tomkiewicz, R. P. Groff, P. Avakian, *J. Chem. Phys.* **1971**, *54*, 4504–4507; c) A. M. Müller, Y. S. Avlasevich, W. W. Schoeller, K. Müllen, C. J. Bardeen, *J. Am. Chem. Soc.* **2007**, *129*, 14240–14250; d) J. J. Burdett, A. M. Müller, D. Gosztola, C. J. Bardeen, *J. Chem. Phys.* **2010**, *133*, 144506; e) J. J. Burdett, D. Gosztola, C. J. Bardeen, *J. Chem. Phys.* **2011**, *135*, 214508; f) J. J. Burdett, C. J. Bardeen, *J. Am. Chem. Soc.* **2012**, *134*, 8597–8607; g) S. T. Roberts, R. E. McAnally, J. N. Mastron, D. H. Webber, M. T. Whited, R. L. Brutchey, M. E. Thompson, S. E. Bradforth, *J. Am. Chem. Soc.* **2012**, *134*, 6388–6400; h) W.-L. Chan, T. C. Berkelbach, M. R. Provorse, N. R. Monahan, J. R. Tritsch, M. S. Hybertsen, D. R. Reichman, J. Gao, X. Y. Zhu, *Acc. Chem. Res.* **2013**, *46*, 1321–1329; i) M. W. B. Wilson, A. Rao, K. Johnson, S. Gélinas, R. di Pietro, J. Clark, R. H. Friend, *J. Am. Chem. Soc.* **2013**, *135*, 16680–16688; j) J. R. Tritsch, W.-L. Chan, X. Wu, N. R. Monahan, X.-Y. Zhu, *Nat. Commun.* **2013**, *4*, 2679; k) Z. Birech, M. Schwoerer, T. Schmeiler, J. Pflaum, H. Schwoerer, *J. Chem. Phys.* **2014**, *140*, 114501; l) T. C. Wu, N. J. Thompson, D. N. Congreve, E. Hontz, S. R. Yost, T. Van Voorhis, M. A. Baldo, *Appl. Phys. Lett.* **2014**, *104*, 193901.
- [8] M. Kytka, A. Gerlach, F. Schreiber, J. Kováč, *Appl. Phys. Lett.* **2007**, *90*, 131911.
- [9] Y.-F. Chang, Z.-Y. Lu, L.-J. An, J.-P. Zhang, *J. Phys. Chem. C* **2011**, *116*, 1195–1199.
- [10] P. Gaweł, C. Dengiz, A. D. Finke, N. Trapp, C. Boudon, J.-P. Gisselbrecht, F. Diederich, *Angew. Chem. Int. Ed.* **2014**, *53*, 4341–4345; *Angew. Chem.* **2014**, *126*, 4430–4434. CCDC-980439 (TcCN) contains the supplementary crystallographic

data for this paper. These data can be obtained free of charge from The Cambridge Crystallographic Data Centre via [www.ccdc.cam.ac.uk/data\\_request/cif](http://www.ccdc.cam.ac.uk/data_request/cif).

- [11] A. Rysanyanskiy, I. Biaggio, *Phys. Rev. B* **2011**, *84*, 193203.
- [12] W.-L. Chan, M. Ligges, X. Y. Zhu, *Nat. Chem.* **2012**, *4*, 840–845.
- [13] M. Kasha, H. R. Rawls, M. A. El-Bayoumi, *Pure Appl. Chem.* **1965**, *11*, 371–392.
- [14] a) L. Ma, K. Zhang, C. Kloc, H. Sun, M. E. Michel-Beyerle, G. G. Gurzadyan, *Phys. Chem. Chem. Phys.* **2012**, *14*, 8307–

8312; b) J. N. Schrauben, J. L. Ryerson, J. Michl, J. C. Johnson, *J. Am. Chem. Soc.* **2014**, *136*, 7363–7373.

- [15] I. Carmichael, G. L. Hug, *J. Phys. Chem. Ref. Data* **1986**, *15*, 1–250.

Received: February 11, 2015

Revised: April 14, 2015

Published online: June 10, 2015